ISSN 2063-5346

BOX BEHNKEN DESIGN BASED FORMULATION OPTIMIZATION AND CHARACTERIZATION OF GALLIC ACID LOADED PHYTOSOMES

Rashita Makkar[1], Tapan Behl[2*], Sukhbir Singh[3*], Neelam Sharma[3], Abhishek Chauhan[4], Hardeep Singh Tuli[5]

Article History: Received: 01.02.2023 **Revised:** 07.03.2023 **Accepted:** 10.04.2023

Abstract

The current investigation aims to synthesize gallic acid (GA) based phytosomes formulation using phosphatidylcholine by solvent evaporation technique with the prime objective of dissolution enhancement of GA. Box-Behnken Design was used to analyze the effect of drug: lipid concentration (X_1), reflux time (X_2) and reflux temperature (X_3) on dependent variables *i.e.* entrapment efficiency (Y_1), yield % (Y_2) and drug loading (Y_3) using Design-expert software. The fourier transform infrared spectroscopy and x-ray diffraction (XRD) studies confirmed the absence of any incompatibilities between the drug-polymer and indicated successful incorporation of GA in optimized phytosome. It was determined that the quadratic model was distinctive to best describe the statistical analysis of GA loaded phytosomes on the basis of its insignificant *p*-value ($p > 0.05$) for lack of fit analysis and significant *p*-value for model ($p < 0.05$). The quadratic equation for response variables were: Y_1= $60.48+15.48X_1-0.4650\ X_2-1.96\ X_3-0.0975X_1X_2+1.90\ X_1X_3-1.54\ X_2X_3+14.35X_1^2-0.9220X_2^2+0.2655X_3^2$; Y_2 = $+55.99+15.43X_1-0.4375X_2-1.98X_3-0.2025X_1X_2+1.69X_1X_3-1.58X_2X_3+14.11X_1^2-0.9450X_2^2 + 0.2225X_3^2$ and $Y_3=15.12-0.8525X_1-0.1062X^2-0.5713X_3+0.0050X_1X_2+0.6400X_1X_3-0.3875X_2X_3+3.81X_1^2-0.2938\ X_2^2+0.1313X_3^2$. The formulation and processing conditions for optimized GAP were 1:3 of drug: lipid (w/w), reflux time of 3.8 hours and reflux temperature of 80°C with desirability function of 0.861. The finalized batch of GA phytosomes showed entrapment efficiency of 91.63%, process yield of 86.65% and drug loading of 18.48%. The study established that phytosomes produced an increase in dissolution of GA by 1.97-fold, 1.63-fold, 1.38-fold and 1.86-fold at 1, 2, 6 and 24 hours, respectively. The *in-vitro* dissolution profile of GAP confirmed that in concurrent to dissolution rate enhancement, the phytosomes demonstrated sustained release pattern till 24 hours. The current research conclusively demonstrated that phytosomes hold an enormous potential role as drug delivery design to enhance the dissolution of phytoconstituents in conjunction with sustained behaviour.

Keywords: Gallic Acid; Phytosome; Box-Behnken Design; Optimization; Desirability Function.

[1]Chitkara College of Pharmacy, Chitkara University, Punjab, India

[2]School of Health Sciences &Technology, University of Petroleum and Energy Studies, Bidholi-248007, Dehradun, Uttarakhand, India

[3]Department of Pharmaceutics, MM College of Pharmacy, Maharishi Markandeshwar (Deemed to be University), Mullana-Ambala, Haryana, India, 133207

[4]Amity Institute of Environmental Toxicology, Safety and Management, Amity University, Noida 201303, India

[5]Department of Biotechnology, Maharishi Markandeshwar Engineering College, Maharishi Markandeshwar (Deemed to be University), Mullana, Ambala 133207, India

Authors for correspondence: tapanbehl31@gmail.com; singh.sukhbir12@gmail.com

DOI: 10.31838/ecb/2023.12.4.170

1. INTRODUCTION

Drug delivery approach consolidates with the formulation of any drug compound and its route of intake. It comprises of innovative technologies which aims to enhance the therapeutic outcome of the active molecule in body by developing formulations which safely transports it[1,2]. Currently, the research is mainly emphasized upon synthesizing drug formulations which exhibits enhanced dissolution profile and sustained release effects within the body, hence increasing its therapeutic efficacy significantly[3,4]. The phytosomes are one of the most common vesicular lipid-based delivery systems which are mainly used to encapsulate plant derived compounds and drugs[5]. They are mainly synthesized by attaching the herbal compound drug with a lipid phosphatidylcholine base eventually resulting in formation of a highly soluble drug formulation with enhanced absorption, pharmacokinetic and pharmacodynamic properties of the drug compounds as compared to original herbal extract[6,7]. The phytosomes are easy to formulate and can be scaled up commercially due to its simple preparation procedure. The technology of phytosomes to encapsulate herbal extracts and polyphenolic compounds have led to origination of nano-formulation which can be efficiently used in management of chronic diseases and promising a bright future for the herbal drug compounds[8, 9]. The rheumatoid arthritis (RA) is an autoimmune chronic inflammatory disorder mainly affecting joints of hands and feet and is highly prominent in older people[10, 11]. With the advancement in technology in research and development sector, rheumatoid arthritis has emerged as one of the most intriguing topics of medicinal research[12]. Several new lead molecules being explored for their therapeutic property are being tested in preclinical, clinical, and post-marketing studies to develop better treatment opportunities for management of this debilitating disorder in patients. *Tecoma stans* belonging to family Bignoniaceae has been identified as promising herbal plant, also renowned by *Bignonia stans, Kuntze seem, Gelseminum stans*[13-15]. The plant presents antibacterial[16], anti-cancer[17], anti-inflammatory[18, 19], antioxidant[20], immunomodulatory, and anti-diabetic properties[21-24] attributed to its phytoconstituents namely tetradecanoic acid, n-nonadecanol, 1-(+)-ascorbic acid 2,6-dihexadecanoate, ellagic acid, gallic acid, octadecanoic acid, etc. Gallic acid (GA) (Figure 1), a polyphenolic compound is found in leaves of *Tecoma stans* which has been reported in treatment of RA as it is a strong antioxidant molecule and possesses immunomodulatory activity, regulates pro-/anti-apoptotic proteins, and inhibits IL-6, which are the chief pathological factors responsible for occurrence and progression of the disease[25]. Despite the wide pharmacological properties of GA, the compound possesses poor dissolution and undergo extensive metabolism which has led to derivation of its phytosome formulation to overcome the challenges it presents and to enhance its efficacy[26]. The phytosome formulation comprises of a drug carrier which is responsible for increasing its aqueous solubility which therefore increases its dissolution profile and also provides sustained release profile. The chemical structure of phosphatidylcholine is presented in Figure 1. Phosphatidylcholine is a bifunctional biodegradable compound which contains lipophilic phosphatidyl moiety and hydrophilic choline moiety. The cholesterol enhances the ability of the active drug to permeate the cell membrane and hence is used in manufacturing the phytosome[27]. The precise analysis of the chemicals indicates that phytosome usually are flavonoid linked molecular compounds which comprise of at least one phosphatidylcholine molecule. The phytosomes protect the plant derived active phytoconstituent from metabolism by gastric enzymes and bacteria in the gut wall, a gastroprotective property attributed to the presence of phosphatidylcholine[28,29]. In present investigation, gallic acid phytosomes (GAP) were synthesized using phosphatidylcholine as lipidic polymer by solvent evaporation technique. Box-Behnken Design (BBD) was used in the study to assess interaction between independent variables independent variables drug: lipid concentration, reflux time (hrs) and reflux temperature (°C) and dependent factors such as entrapment efficiency, yield and drug loading with each other and thereby develop the best optimized batch containing composition and conditions which best suit the process of production of GAP.

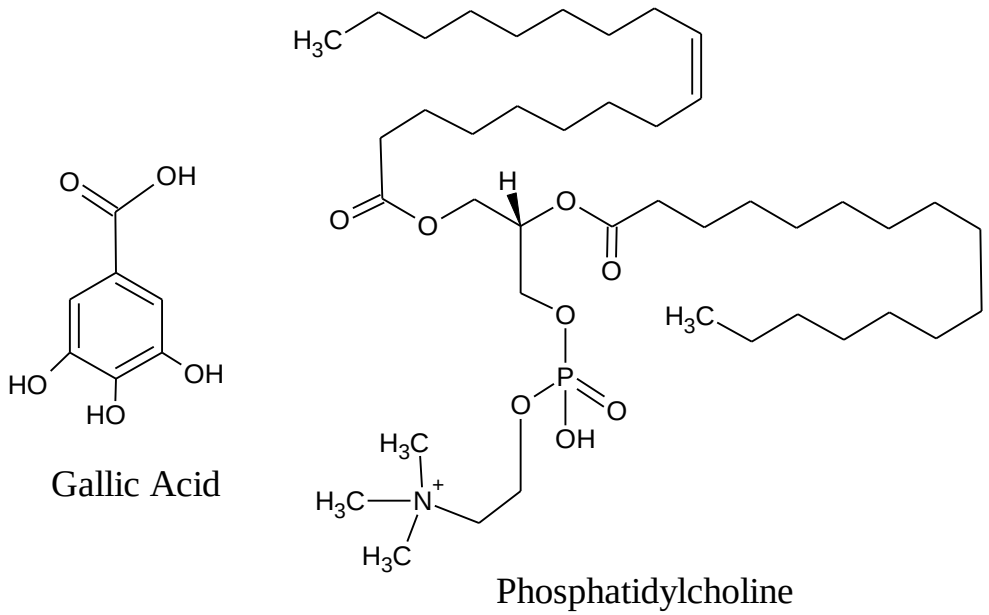

Figure 1. Chemical structure of gallic acid and phosphatidylcholine

2. MATERIALS AND METHODS

2.1. Materials

Gallic acid (3,4,5-trihydroxy benzoic acid, $C_7H_6O_5$) was isolated from hydroalcoholic extract of *Tecoma stans* leaves from Chemical Resources (Chereso), Industry, Pvt. Ltd, India. Phosphatidylcholine was obtained from Himedia, Mumbai. Dimethyl sulfoxide [$(CH_3)_2SO_2$, molecular weight: 94.13], and dichloromethane [CH_2Cl_2, Molecular weight: 84.93] were procured from Loba chemicals, Mumbai, India. All the chemicals used in the current study were of analytical grade.

2.2. Methods

2.2.1. Experimental design

Box-Behnken Design (BBD) has been employed in the current study to synthesise seventeen batches of GAP to find the best possible optimised batch of phytosomes by investigating the interactions between independent and dependent variables as mentioned in Table 1. The design layout of GAP batches is specified in Table 2. The design mainly studies the interaction and quadratic effects of factors on the dependent variables which is further utilised in the synthesising the optimized formulation[30]. The design generated below quadratic model equation:

$$Y = B_0+B_1X_1+B_2X_2+B_3X_3+B_4X_1X_2+B_5X_1X_3+B_6X_2X_3+B_7X_1^2+B_8X_2^2+B_9X_3^2$$

Y being characterized as a dependent variable, B_0 to B_9 is characterized as the regression coefficients of respective independent variables and their associated interaction terms. The independent variables have been presented as X_1, X_2 and X_3. The interaction and quadratic terms are expressed by X_1X_2 and X_i^2, where i=1, 2, 3 respectively. The current study evaluates drug/polymer ratio (w/w), reflux time (h) and reflux temperature (°C), all parameters taken in low, medium and high concentrations. The entrapment efficiency (% w/w), yield (% w/w) and drug loading (% w/w) were dependent variables.

Table 1: The variables and their levels used in production of gallic acid phytosomes

Independent Variables	**Coded Levels of Variables**		
	–1	0	+1
X_1= Drug: Lipid (w/w)	1:1	1:2	1:3
X_2= Reflux Time (Hrs)	2	3	4
X3= Reflux Temperature (°C)	60	70	80
Dependent Variables	**Constraints**		
Y_1= Entrapment Efficiency (% w/w)	Maximize		
Y_2= Yield (% w/w)	Maximize		
Y_3= Drug loading (% w/w)	Maximize		

Table 2: Experimental layout for 3 factors 3 levels Box-Behnken Design

Run	**X_1: Drug: Lipid (w/w)**	**X_2: Reflux Time (hrs)**	**X3: Reflux Temperature (°C)**
1	-1	-1	0
2	1	-1	0
3	-1	1	0
4	1	1	0
5	-1	0	-1
6	1	0	-1
7	-1	0	1
8	1	0	1
9	0	-1	-1
10	0	1	-1
11	0	-1	1
12	0	1	1
13	0	0	0
14	0	0	0
15	0	0	0
16	0	0	0
17	0	0	0

2.2.2. Fabrication of gallic acid phytosomes

Gallic acid phytosomes were prepared by solvent evaporation technique[31]. In brief, GA was dissolved in dimethyl sulfoxide while cholesterol and phosphatidylcholine were dissolved in dichloromethane. Subsequently, these solutions were transferred in round bottom flask which was refluxed at different temperatures and time periods as mentioned in Table 1 to achieve formation of phytosomes. The concentrated product was further evaporated under vacuum to remove solvent and finally, the phytosomes were collected for further studies.

2.2.3. Evaluation of gallic acid phytosomes

2.2.3.1. Determination of entrapment efficiency (Y_1)

The amount of drug entrapped was studied for all the batches of phytosomes[32]. The product weighing 100 mg was transferred into a volumetric flask which contains 100 ml quantity of phosphate buffer pH 6.8 and was placed aside. The volumetric flask on the following day was continuously stirred for 2 hours at a temperature of 37±2°C to ensure that the entire drug was successfully release from the formulation. The solution formed was filtered and 1 ml of the filtered solution was further diluted to up to 10 ml for analyzing the entrapment efficiency of the formulation in UV spectrophotometer at 262 nm. The formula used for calculation of drug entrapment is depicted in equation 1.

$$\text{Drug Entrapment Efficiency (\%)} = \frac{\text{Actual content of drug}}{\text{Theoretically calculated amount of drug}} \times 100 \quad \text{Eq. 1}$$

2.2.3.2. Determination of % yield (Y_2)

The percentage yield of drug was obtained by drying and weighing the phytosomes accurately. The weight obtained was further divided with the total weight of the combination of non-volatile excipients and the drug[33]. The equation 2 was used for calculation of percentage yield.

$$\text{\% Yield} = \frac{\text{Total weight of phytosomes}}{\text{Total weight of drug and excipients}} \times 100 \quad \text{Eq. 2}$$

2.2.3.3. Determination of % drug loading (Y_3)

The % drug loaded within the prepared phytosomes was determined by transferring the weighed product into volumetric flask containing 100 ml phosphate buffer pH 6.8 and was placed aside. The volumetric flask was continuously stirred at 37±2°C for 2 hours on the following day to ensure that the entire drug was release from the formulation. The solution was filtered and 1ml of filtered solution was further diluted to 10 ml to analyze under UV spectrophotometer for assessing the loaded drug amount at 262 nm[34]. The drug loaded was calculated by the formula mentioned in equation 3.

$$\text{Drug loading (\%)} = \frac{\text{Actual content of drug}}{\text{Theoretically calculated amount of drug+lipids}} \times 100 \quad \text{Eq. 3}$$

2.2.4. Optimization and validation of gallic acid phytosomes

The polynomial equations were statistically validated *via* assessing statistical factors like correlation coefficient and *p*-value which were obtained from ANOVA functionality available in the design expert software. The graphical optimization tool within the design-expert software was used to determine optimum values of the variables based on the set constrained criteria[35].

2.2.5. Fourier transform infrared spectroscopy (FTIR)

The spectrum derived by FTIR of GA, phosphatidylcholine, cholesterol, physical mixture and GAP were obtained through FTIR spectrophotometer (Shimadzu, Germany)[36]. Samples were collected and mixed with powder of 1% potassium bromide, thereafter, is pressed to self-support the disks. The spectrums were scanned within the analytical range of 400 to 4000 cm^{-1}.

2.2.6. X-ray diffraction (XRD)

XRD patterns of GA, phosphatidylcholine, cholesterol, physical mixture and GAP was extracted on an X-ray diffractor (X'pert Pro diffractometer) by using a 10 mm specimen at a temperature of 25°C at 1.54A° Cu Kα radiation and 1.39 A° Cu Kβ radiation (operated by tube at 45kV, 40 mA). The data was gathered at an angular range from 2θ=5° to 2θ=50° in a continuous scanning mode[37].

2.2.7. Scanning electron microscopy (SEM)

The surface morphology of GAP prepared *via* optimization design expert software was analyzed with the help of SEM technique by using scanning electron microscope (Hitachi S3400 N) of variable pressure. The phytosomes were plated with gold palladium for 150 seconds and a 20 nm film was achieved for examination under the atmosphere of air (Coater Polaron, 18mA current at 1.4kV)[38].

2.2.8. *In-vitro* drug release study

The process of determination of release of drug from the optimized GAP was conducted *via* dissolution of drug product in pH 6.8 phosphate buffer, 100 revolutions per minute at 37 ±0.5°C for

24 hours by using USP dissolution paddle apparatus (n=3). The samples were taken at definite time intervals of 0.5, 1, 2, 4, 6, 8, 12 and 24 hours which were further analyzed with the help of spectrophotometer at 262 nm[39-41].

2.3. Statistical analysis

The results obtained were presented as mean value ±standard deviation and ANOVA present in the design expert software was used to statistically analyze the data. *In-vitro* data was analyzed by ANOVA for significance followed by Bonferroni post-test for comparison of average values[42]. The difference showing $p < 0.05$ statistically was considered significant.

3. RESULTS AND DISCUSSION

3.1. Selection of appropriate design model for Y1 to Y3

The differences in the values of adjusted and predicted r^2 for the quadratic model was less than 0.2, *p*-value was greater than 0.05 for lack-of fit while the sequential *p*-value was less than 0.05, indicating the precision of quadratic model for assessment of dependent variables as presented in Table 3.

Table 3: Design model for estimation of best fit model for Y_1-Y_3 of gallic acid phytosomes

Source	Y	R^2	Adjusted R^2	Predicted R^2	LOF p-value	Sequential *p*-value
Linear	Y_1	0.6824	0.6091	0.4063	0.0001	0.0015
	Y_2	0.6891	0.6174	0.4181	< 0.0001	0.0013
	Y_3	0.1161	-0.0878	-0.6541	< 0.0001	0.6449
2FI	Y_1	0.6909	0.5054	-0.2931	< 0.0001	0.9634
	Y_2	0.6968	0.5148	-0.2718	< 0.0001	0.9671
	Y_3	0.1467	-0.3653	-2.5694	< 0.0001	0.9467
Quadratic	Y_1	0.9958	0.9903	0.9468	0.0965	< 0.0001
	Y_2	0.9961	0.9911	0.9496	0.0807	< 0.0001
	Y_3	0.9865	0.9691	0.8192	0.0575	< 0.0001
Cubic	Y_1	0.9990	0.9960	-	-	0.0965
	Y_2	0.9992	0.9966	-	-	0.0807
	Y_3	0.9976	0.9902	-	-	0.0575

3.2. Statistical assessment of variables by Design-Expert Software

3.2.1. Entrapment efficiency (Y_1)

The variation between the adjusted and predicted r^2 values *i.e.*, 0.9903 and 0.9468 respectively was found to below 0.2 as per fit summary statistics. The lack of fit (LOF) *p*-value for Y_1 was obtained as 0.0965 ($p > 0.05$) (Table 4), suggesting that insignificance in the LOF *p*-value presents good fitting of the model. Quadratic design was concluded to be the best fit was Y_1.

Y_1 was found to be significantly impacted by changes in the drug: lipid (X_1) with *p*-value < 0.0001 and reflux temperature (X_3) with *p*-value 0.0039 as principal effect ($p < 0.05$) and effect of interaction between X_1 and X_3 with *p*-value 0.0230 was also found significant which indicated synergistic combined effect ($p < 0.05$). The review of literature from previous researches also revealed the significant effect of drug: lipid concentration and reflux temperature on entrapment efficiency[43-48]. Furthermore, quadratic impact of X_1^2 on Y_1 was found to be significant with *p*-value < 0.0001 ($p< 0.05$).

Quadratic equation 4 showed that drug: lipid (X_1) produced synergistic effect on Y_1 (b_1= 15.48) and reflux time (X_2) and reflux temperature (X_3) (b_2 = -0.4650; b_3 = -1.96) showed antagonistic effect. This showed that increasing the amount of X_1 in GAP enhanced the value of Y_1 which is also reflected in response surface plots (Figure 2).

Y_1= 60.48 +15.48X_1-0.4650 X_2-1.96 X_3-0.0975 X_1X_2+1.90 X_1X_3 -1.54 X_2X_3 +14.35 X_1^2-0.9220 X_2^2 +0.2655 X_3^2 Eq. (4)

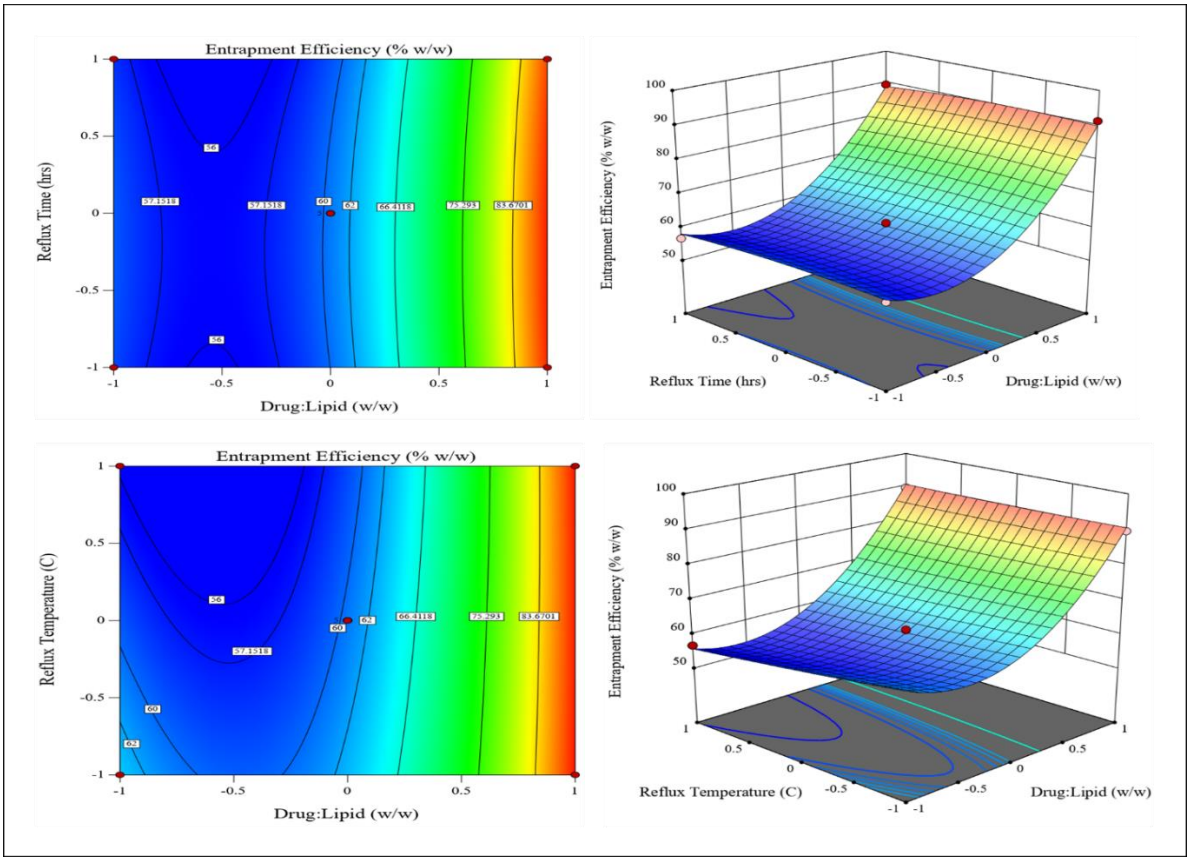

Figure 2. Contour plots and response surface plots showing effect of independent parameters on entrapment efficiency of gallic acid phytosomes

Table 4. Analysis of variance of gallic acid phytosomes for dependent variable (Y_1)

Source	Sum of Squares	Df	Mean Square	F-value	p-value
Model	2844.25	9	316.03	183.04	< 0.0001
X_1	1916.73	1	1916.73	1110.12	< 0.0001
X_2	1.73	1	1.73	1.00	0.3502
X_3	30.77	1	30.77	17.82	0.0039
X_1X_2	0.0380	1	0.0380	0.0220	0.8862
X_1X_3	14.52	1	14.52	8.41	0.0230
X_2X_3	9.52	1	9.52	5.51	0.0513
X_1^2	866.50	1	866.50	501.85	< 0.0001
X_2^2	3.58	1	3.58	2.07	0.1931
X_3^2	0.2968	1	0.2968	0.1719	0.6908
Lack of fit	9.22	3	3.07	4.30	0.0965

3.2.2. Percentage yield (Y_2)

The variation between adjusted and predicted r^2 values 0.9911 and 0.9496 respectively was evaluated as less than 0.2 on the basis of fit summary characteristics (Table 5). The LOF *p*-value for $Y_2$was found 0.0807 ($p > 0.05$). The insignificance in LOF *p*-value indicated good fitting of the model and hence the quadratic design was evaluated as the best fir for Y_2.

Y_2 was substantially impacted by drug: lipid (X_1) with *p*-value < 0.0001 and reflux temperature (X_3) with *p*-value 0.0029 as principal effect ($p< 0.05$) and the effects of interactions between X_1 and X_3 with *p*-value 0.0311; X_2 and X_3 with *p*-value 0.0395 was also found significant which indicated synergistic combined effect ($p< 0.05$). Furthermore, the quadratic effect of X_1^2 on Y_2 was also found significant with *p*-value < 0.0001 ($p < 0.05$). The review of literature from previous researches also demonstrated the significant effect of drug: lipid concentration and reflux temperature on percentage yield [49-53].

The second polynomial equation (Eq. 5) indicates that X_1 expressed synergistic effect on Y_2 (b1= 15.43). This showed that increasing the amount of X_1 enhanced the value of Y_2 which is also reflected in response surface plots (Figure 3).

$$Y_2 = 55.99+15.43\ X_1-0.4375\ X_2-1.98\ X_3-0.2025\ X_1X_2+1.69\ X_1X_3-1.58\ X_2X3+14.11\ X_1^2-0.9450\ X_2^2+0.2225\ X_3^2 \quad \text{Eq. (5)}$$

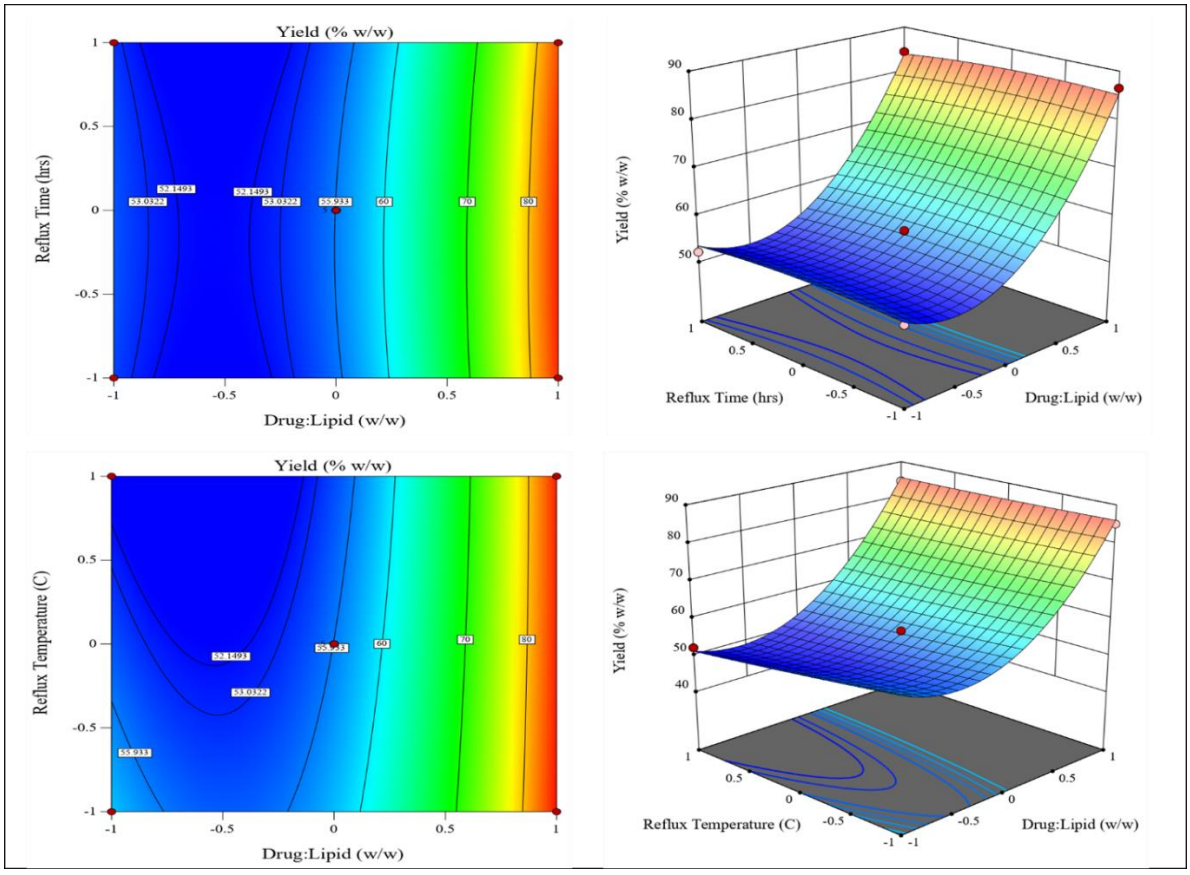

Figure 3. Contour plots and response surface plots showing effect of independent parameters on percentage yield of gallic acid phytosomes

Table 5. Analysis of variance for yield (Y_2) of gallic acid phytosomes

Source	Sum of Squares	Df	Mean Square	F-value	p-value
Model	2802.09	9	311.34	198.22	< 0.0001
X_1	1905.61	1	1905.61	1213.25	< 0.0001
X_2	1.53	1	1.53	0.9749	0.3564
X_3	31.40	1	31.40	19.99	0.0029
X_1X_2	0.1640	1	0.1640	0.1044	0.7560

X_1X_3	11.36	1	11.36	7.23	0.0311
X_2X_3	10.02	1	10.02	6.38	0.0395
X_1^2	837.99	1	837.99	533.52	< 0.0001
X_2^2	3.76	1	3.76	2.39	0.1657
X_3^2	0.2084	1	0.2084	0.1327	0.7264
Lack of fit	8.62	3	2.87	4.85	0.0807

3.2.3. Percentage drug loading (Y_3)

The difference between adjusted r^2 (0.9691) and predicted r^2 (0.8192) was below 0.2 as per fit summary statistics. The LOF *p*-value for Y_3 was found 0.0575 ($p > 0.05$) (Table 6). Insignificance in LOF *p*-value indicated a good fitting of the model and also concluded that the quadratic design was the best fit for Y_3.

Y_3 was substantially influenced by drug: lipid (X_1) with *p*-value 0.0004 and reflux temperature (X_3) with *p*-value 0.0036 as the chief effect ($p < 0.05$) and the effect of relation between X_1 and X_3 with *p*-value 0.0114 was also found significant which indicated synergistic combined effect ($p < 0.05$). Furthermore, the quadratic effect of X_1^2 on Y_1 was also found significant with *p*-value < 0.0001 ($p< 0.05$). The review of literature from previous researches also illustrated the significant effect of drug: lipid concentration and reflux temperature on drug loading[54-57].

From polynomial equation 6, it has been revealed that X_1, X_2 and X_3 produced synergistic effect on Y_3 (b_1= -0.8525; b_2 = -0.1062; b_3= -0.5713). This is also revealed in response surface plots (Figure 4).

$$Y_3= +15.12-0.8525\ X_1-0.1062\ X_2\ -0.5713\ X_3+0.0050\ X_1X_2\ +0.6400\ X_1X_3\ -0.3875\ X_2X_3+3.81\ X_1^2\ -0.2938\ X_2^2\ +0.1313\ X_3^2 \quad \text{Eq. (6)}$$

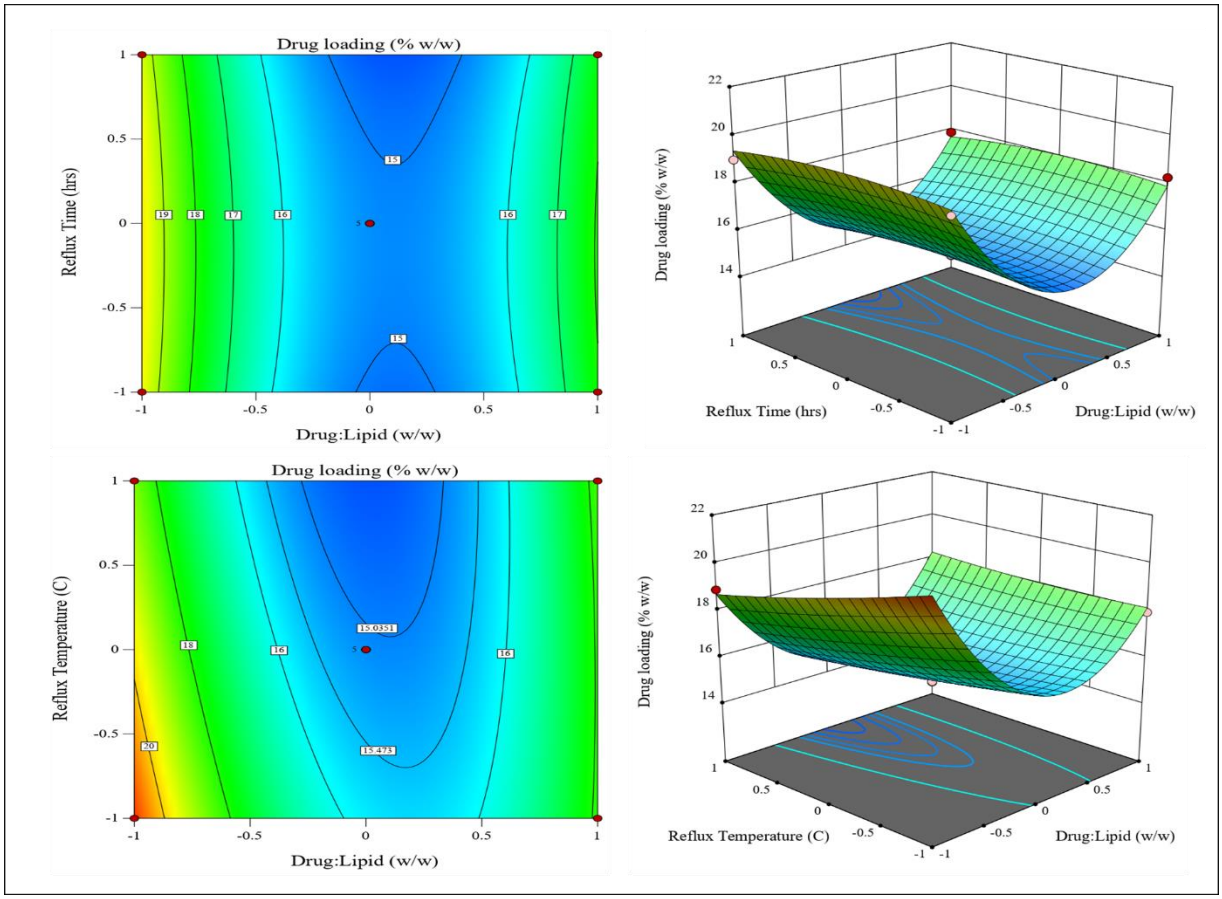

Figure 4. Contour plots and response surface plots showing effect of independent parameters on percentage drug loading of gallic acid phytosomes

Table 6. Analysis of variance for drug loading (Y_3) of gallic acid phytosomes

Source	Sum of Squares	Df	Mean Square	F-value	p-value
Model	72.32	9	8.04	56.83	< 0.0001
X_1	5.81	1	5.81	41.11	0.0004
X_2	0.0903	1	0.0903	0.6387	0.4505
X_3	2.61	1	2.61	18.46	0.0036
X_1X_2	0.0001	1	0.0001	0.0007	0.9795
X_1X_3	1.64	1	1.64	11.59	0.0114
X_2X_3	0.6006	1	0.6006	4.25	0.0783
X_1^2	61.08	1	61.08	431.94	< 0.0001
X_2^2	0.3633	1	0.3633	2.57	0.1530
X_3^2	0.0725	1	0.0725	0.5129	0.4971
Lack of fit	0.8109	3	0.2703	6.04	0.0575

3.3. Optimization and validation of optimized GAP by numerical optimization method

The optimal values of optimized GAP were 1:3 of drug: lipid (w/w), reflux time of 3.8 hours and reflux temperature of 80°C was explored by Design expert software which has desirability function of 0.861 (Figure 5). The evaluation between the experimental and predicted values of the dependent variables of the optimized GAP batch confirmed the authenticity of the power of prediction of the model as suggested by a percent bias value which was smaller than 5% (Table 7).

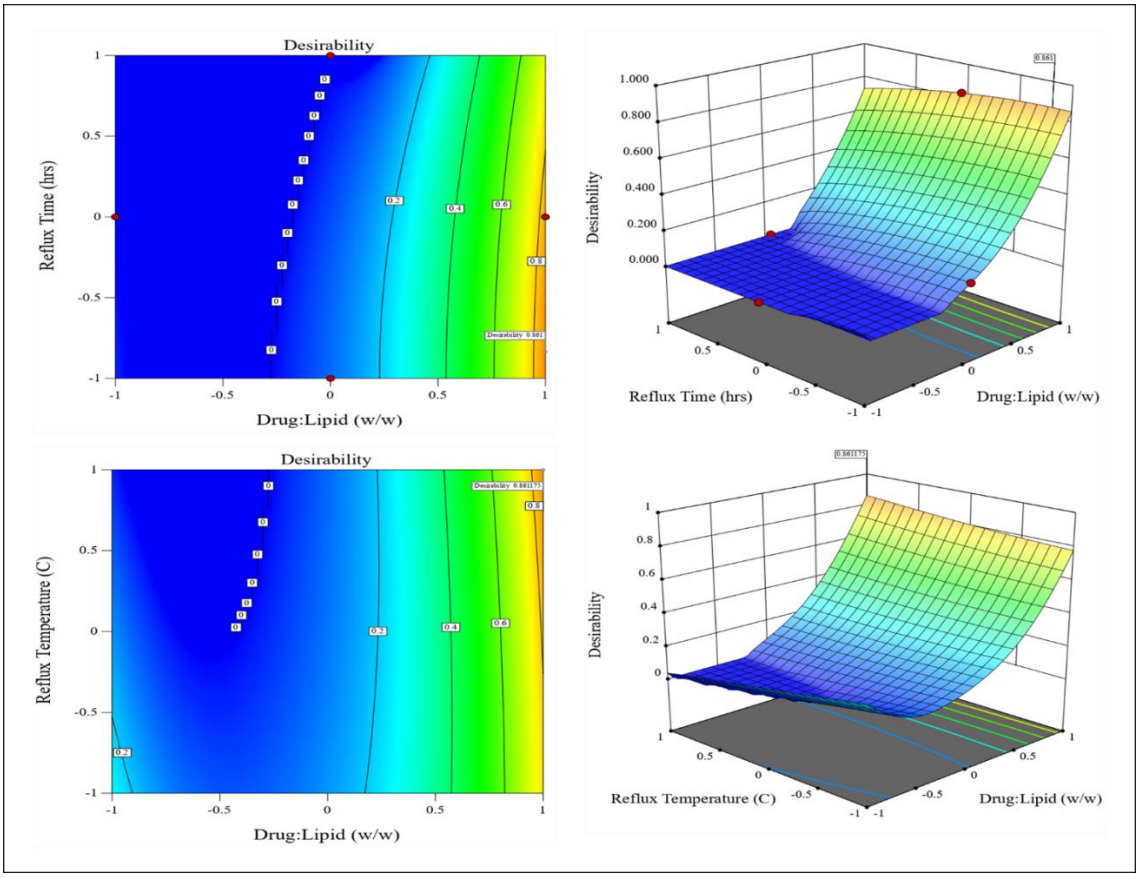

Figure 5. Contour plots and corresponding response surface plots for desirability function of optimized gallic acid phytosomes

Table 7. The experimental *versus* predicted values of response parameters for optimized gallic acid phytosomes

Response variables	Predicted value	Experimental value	Bias (%)
Y_1= Entrapment Efficiency (% w/w)	91.63	90.48	1.25
Y_2= Yield (% w/w)	86.65	85.34	1.51
Y_3= Drug Loading (% w/w)	18.48	17.67	4.38

3.4. Characterization of GAP phytosomes

3.4.1. Fourier transform infrared spectroscopy

The FTIR spectrum of GA, cholesterol, Phosphatidylcholine, physical mixture and GAP are shown below in Figure 6. The absorption peaks of GA were determined at 3495 cm^{-1}, 1703 cm^{-1}, and 1541 cm^{-1} correspond to C=C, C=O, O-H, of alkene stretch and aromatic ring respectively confirming the legitimacy of the compound. The chief absorption peaks of GAP were found to be present in the physical mixture indicating lack of interaction between the drug and lipid polymer. The chief absorption peaks of GAP were found to be present in the physical mixture indicating lack of interaction between the drug and lipid polymer. The comparison between gallic acid and GAP showed that the peaks 3065 cm^{-1}, 3005 cm^{-1}, 2926 cm^{-1} present in gallic acid have shifted in GAP indicating the formation of phyto phospholipid complexes[58, 59].

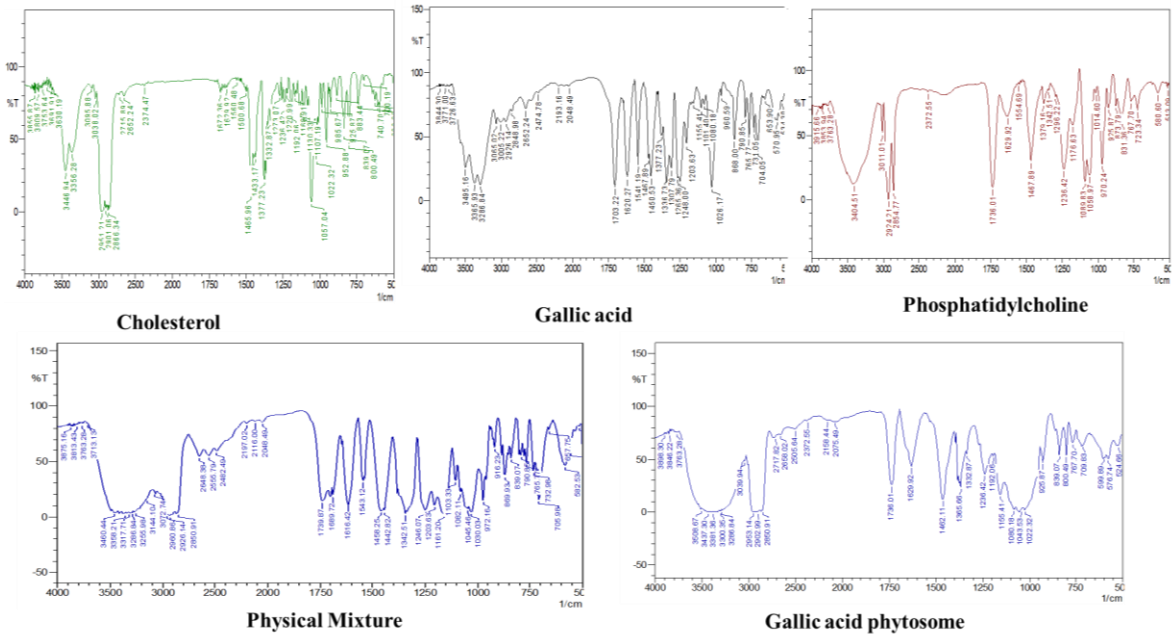

Figure 6. Fourier transform infrared spectra of cholesterol, gallic acid, phosphatidylcholine and physical mixture, and gallic acid phytosomes

3.4.2. Powder x-ray diffraction (PXRD)

The prominent PXRD peaks of samples are shown in Table 8. The Figure 7 (a) below represents GA which has been shown to possess sharp crystalline peaks at 2θ=16.5°, 2θ=16.6°, 2θ=19.5°, 2θ= 8.0° and 2θ=33.1°. Figure 7(b) represents phosphatidylcholine which shows sharp crystalline peaks at 2θ=15.5°, 2θ=16.3°, 2θ=17.1, 2θ=24.2, and 2θ= 17.7. Figure 7 (c) shows sharp crystalline peaks represented by cholesterol at 2θ=5.2°, 2θ=16.5°, 2θ=14.9° and 2θ=18.4°. Physical mixture, as shown in Figure 7 (d) shows sharp crystalline peaks at 2θ=5.3°, 2θ= 17.1°, 2θ=20.4°, 2θ=5.4° and 2θ=18.1°. GAP exhibited insignificant peaks in the XRD pattern of the GAP as shown in Figure 7 (e).

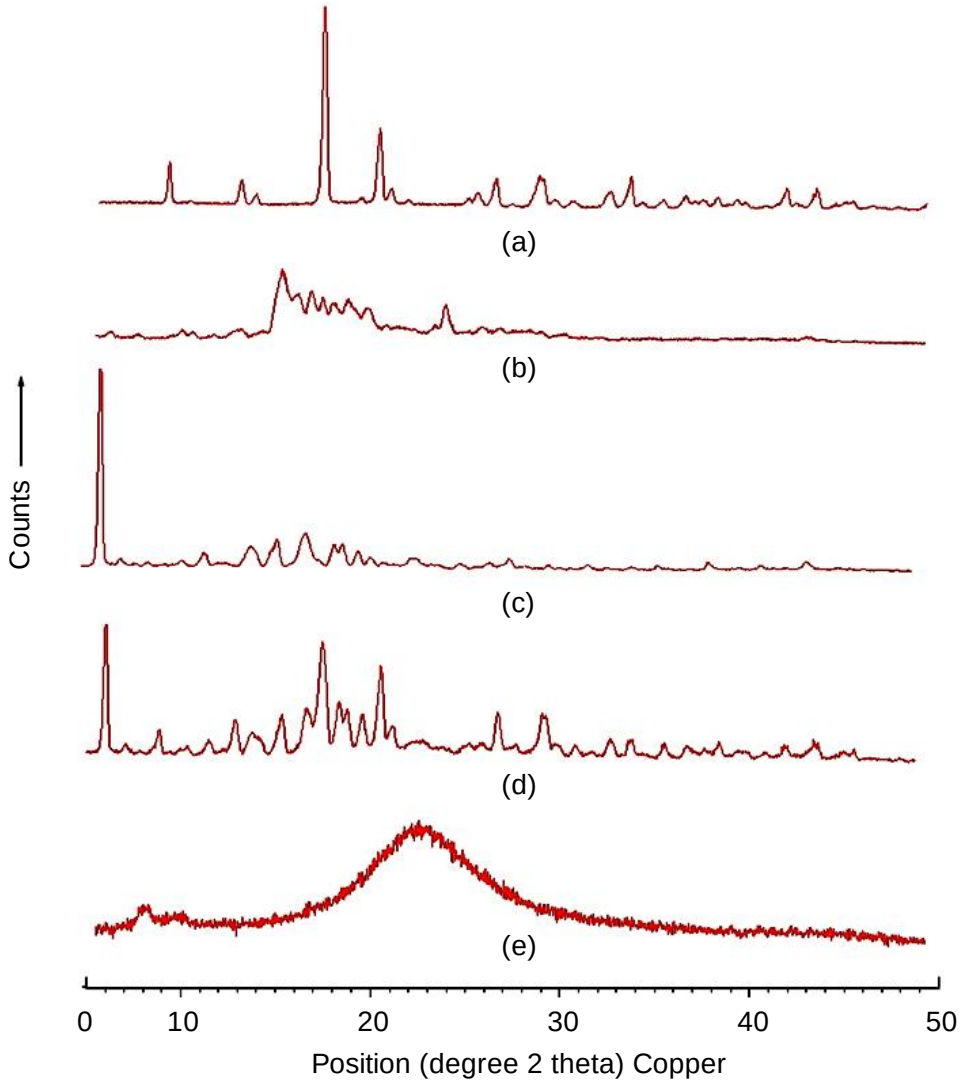

Figure 7. X-ray diffraction pattern of (a) gallic acid, (b) phosphatidylcholine, (c) cholesterol, (d) physical mixture, (e) gallic acid phytosomes

Table 8. Prominent x-ray diffraction peaks observed in XRD pattern of gallic acid, phosphatidylcholine, cholesterol, physical mixture, and gallic acid phytosomes

Pos. [°2θ]	FWHM Total [°2θ]	d-spacing [Å]	Rel. Int. [%]	Area [cts*°2θ]
Gallic acid				
8.0894	0.2093	10.92087	26.06	225.52
12.0138	0.2840	7.36086	14.42	155.76
16.5234	0.2882	5.36066	100.00	1242.87
16.6217	0.1437	5.32917	47.44	252.70
19.5380	0.3016	4.53981	46.44	586.93
25.8588	0.3140	3.44267	16.70	202.40
28.1679	0.5184	3.16548	13.91	288.96
33.1879	0.3393	2.69724	17.06	269.80
43.3605	0.1643	2.08512	15.55	189.21
Phosphatidylcholine				
15.5612	0.7398	5.68989	41.12	970.68
16.3931	0.6299	5.40298	25.36	550.72
17.1161	0.4287	5.17634	23.24	381.02
17.7054	0.4615	5.00535	19.47	570.90

18.3221	0.5716	4.83824	14.65	495.01
19.0591	0.5392	4.65279	15.99	441.04
20.1187	0.5872	4.41006	14.05	319.29
24.2036	0.3654	3.67422	19.51	333.51
Cholesterol				
5.2958	0.2429	16.67374	100.00	1982.24
14.9369	0.2811	5.92626	10.73	227.69
16.5720	0.5534	5.34507	11.55	876.09
18.4668	0.3614	4.80068	10.53	308.44
Physical Mixture				
5.3178	0.2291	16.60483	100.00	431.29
5.4284	0.1284	16.26671	48.35	96.95
12.4259	0.3597	7.11764	31.09	219.53
14.9133	0.4532	5.93560	31.47	222.65
16.3857	0.5862	5.40540	41.06	464.88
17.1797	0.5082	5.15732	78.81	625.20
17.3164	0.1408	5.11691	34.36	150.93
18.1074	0.4071	4.89512	42.41	269.45
18.5718	0.3385	4.77377	38.49	253.43
19.3822	0.3945	4.57595	33.59	245.19
20.2570	0.3129	4.38028	38.85	297.96
20.4474	0.2356	4.33991	62.84	291.79
21.0177	0.3814	4.22343	22.16	132.74
26.8001	0.3275	3.32385	37.82	238.36
29.2268	0.3337	3.05316	37.97	362.35
29.4682	0.2033	3.02869	20.76	65.89
Gallic acid phytosomes				
6.8945	0.7944	12.81057	100.00	62.20
8.5499	1.5232	10.33369	43.06	49.41
39.0056	0.0900	2.30730	20.16	1.66
40.5211	0.4015	2.22628	30.08	8.17

3.4.3. Scanning electron microscopy (SEM)

The SEM studies helped in determining the texture and morphological surface of the phytosomes. SEM studies revealed that the phytosomes were having rough morphology along with elongated forms with loosely bound together (Figure 8). The SEM results from previous researches also support this[60-62].

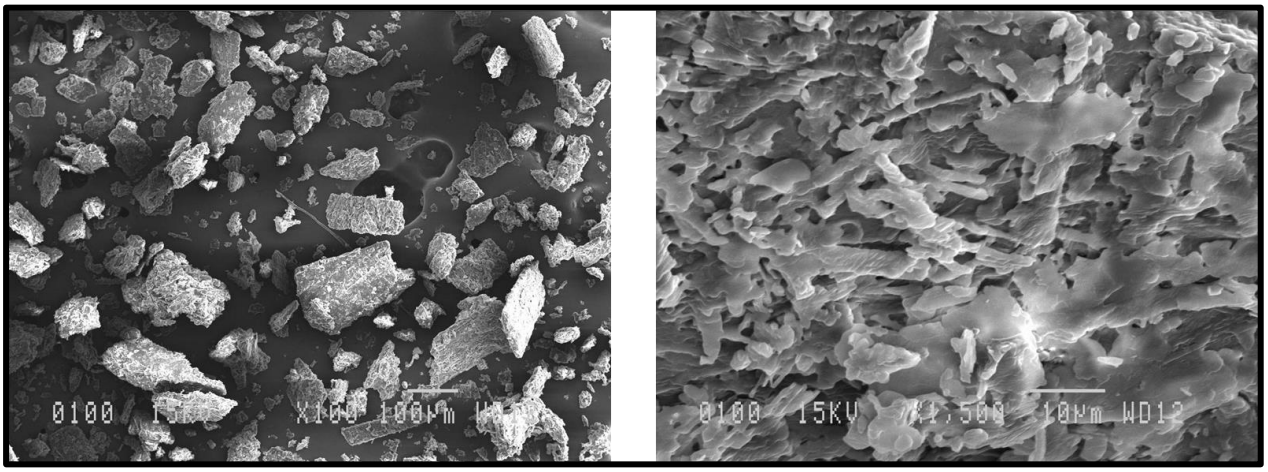

Figure 8. Scanning electron microscopy images of gallic acid phytosomes

3.5. *In-vitro* drug release profile from optimized GAP

Gallic acid, physical mixture, and GAP optimized batch exhibited percentage cumulative drug release of 15.32%, 17.75% and 30.19% within 1 hour respectively,25.43%, 31.28% and 41.53% within 2 hours respectively, 46.38%, 48.21% and 64.35% within 6 hour respectively, 46.29%, 48.41% and 86.37% within 24 hour respectively which indicated that the dissolution of gallic acid was enhanced 1.97-fold, 1.63-fold, 1.38-fold and 1.86-fold at 1, 2, 6 and 24 hours respectively, which can be attributed to the solubilization of GA due to formation of phytosomes (Figure 9). GAP presented low dissolution as the drug was floating on the phosphate buffer pH 6.8 buffer due to hydrophobic characteristics. The improvement in dissolution of GA was due to enhancement in its solubility profile due to formation of phytosomes[63,64]. Apart from enhancement in dissolution rate, this was observed that GAP exhibited sustained release profile till 24 hours which is attributable to the entrapment of GA in phosphatidylcholine.

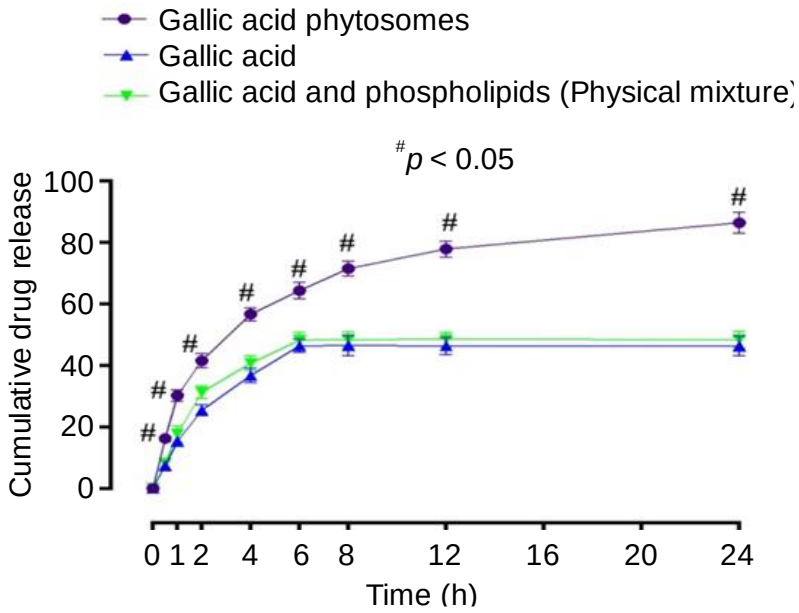

Figure 9. *In-vitro* drug release profile of gallic acid phytosomes in comparison to plain gallic acid and physical mixtures

4. CONCLUSIONS

Gallic acid is a strong antioxidant molecule and comprises several therapeutic properties such as anti-inflammatory, antibacterial, anticancer, and immunomodulatory. The drug has therapeutic value but has poor dissolution along with extensive metabolism. To overcome the aforesaid challenge, phytosomes of active drug constituent were manufactured to enhance its dissolution, hence increasing its therapeutic efficacy in patients. In the current study, the phytosomes of gallic acid were prepared by using phosphatidylcholine *via* solvent evaporation technique. The optimized batch of the GAP formed was further analyzed by Box Behnken design to analyze the effect of independent variables like drug: lipid concentration, reflux time and reflux temperature on dependent variables *i.e.* entrapment efficiency, drug loading and percentage yield. The formulation and processing conditions for optimized GAP were 1:3 of drug: lipid (w/w), reflux time of 3.8 hours and reflux temperature of 80°C which was estimated by Design expert software with desirability function of 0.861. The predicted responses for dependent variables were 91.63% for entrapment efficiency, 86.65% for percentage yield and 18.48% for drug loading which were closer to the actual experimental values of 90.48%, 85.34% and 17.67% for entrapment efficiency, percentage yield and drug loading, respectively. The comparison of experimental and model predicted values of response variables for optimized GAP validated the authenticity of predictive power

of designed model as indicated by % bias value was < 5%. The study also showed that the dissolution of drug increased up to 1.97-fold, 1.63-fold, 1.38-fold and 1.86-fold at 1, 2, 6 and 24 hours, respectively upon formation of phytosomes. The dissolution profile of GAP affirmed that in concurrent to dissolution amplification, the phytosomes exhibited sustained release pattern till 24 hours. Therefore, the research concluded that phytosomes have an enormous potential as a drug delivery approach to increase the dissolution of herbal extract compounds along with sustained behaviour.

ACKNOWLEDGMENTS

The authors acknowledge Chitkara College of Pharmacy, Chitkara University, Punjab, India and Department of Pharmaceutics, MM College of Pharmacy, Maharishi Markandeshwar (Deemed to be University), Mullana-Ambala, Haryana, India 133207 and School of Health Science, University of Petroleum and Energy Studies, Dehradun, Uttarakhand, India for providing platform required for compilation of review.

CONFLICT OF INTEREST

The authors declare no conflict of interest.

REFERENCES

[1] Singh S, Singla Y, Arora S. Development and statistical optimization of nefopam hydrochloride loaded nanospheres for neuropathic pain using Box–Behnken design. *Saudi Pharm J*. **2016,** *24(5)*, 588-99.

[2] Patel J, Patel R, Khambholja K, Patel N. An overview of phytosomes as an advanced herbal drug delivery system. *Asian J Pharm Sci*. **2009,** *4(6)*, 363-71.

[3] Choubey A. Phytosome-A novel approach for herbal drug delivery. *Int. J. Pharm. Sci. Rev. Res*. **2011,** *2(4)*, 807.

[4] Kumar D, Vats N, Saroha K, Rana AC. Phytosomes as emerging nanotechnology for herbal drug delivery. *Sustainable Agriculture Reviews 43*: Pharmaceutical Technology for Natural Products Delivery Vol. 1 Fundamentals and Applications. **2020,** 217-37.

[5] Gao J, Karp JM, Langer R, Joshi N. The future of drug delivery. *Chem. Mater*. **2023,** *35(2)*, 359-63.

[6] Patel PM, Modi CM, Patel HB, Patel UD, Ramchandani DM, Patel HR, Paida BV. Phytosome: an emerging technique for improving herbal drug delivery. *J. Phytopharm*. **2023**; 12(1): 51-58.

[7] Alenzi AM, Albalawi SA, Alghamdi SG, Albalawi RF, Albalawi HS, Qushawy M. Review on different vesicular drug delivery systems (VDDSs) and their applications. *Recent Pat. Nanotechnol*. **2023,** *17(1)*, 18-32.

[8] Dodle T, Mohanty D, Tripathy B, Panigrahy AB, Sirikonda S, Kumar L, Kumar CP, Gobinath M, Patro CS, Bakshi V, Maharana P. A critical review on phytosomes: advancement and research on emerging nanotechnological tools. *CurrBioact Compd*. **2023**, *19(5)*,89-99.

[9] Sharma N, Singh S, Laller N, Arora S. Application of central composite design for statistical optimization of *Trigonella foenum-graecum* phytosome-based cream. *RJPT*. **2020**, *13(4)*, 1627-32.

[10] Makkar R, Behl T, Kumar A, Nijhawan P, Arora S. Emerging therapeutic effects of herbal plants in rheumatoid arthritis. *Endocr. Metab. Immune Disord. - Drug Targets (Formerly Current Drug Targets-Immune, Endocrine & Metabolic Disorders)*. **2021**, *21(4)*, 617-25.

[11] Makkar R, Behl T, Bungau S, Kumar A, Arora S. Understanding the role of inflammasomes in rheumatoid arthritis. *Inflammation*. **2020**, *43*, 2033-47.

[12] Behl T, Makkar R, Arora S. Exploring the effect of *Terminalia catappa* fruit extract in rheumatoid arthritis: an evaluation of behavioural, hematologiocal and histopathological parameters. *EndocrMetab Immune Disord Drug Targets (Formerly Current Drug Targets-Immune, Endocrine & Metabolic Disorders)*.**2021**, *21(6)*, 1073-82.

[13] Anand M, Basavaraju R. A review on phytochemistry and pharmacological uses of *Tecoma stans* (L.) Juss. ex Kunth. *J. Ethnopharmacol*.**2021,** *265*, 113270.

[14] Bargah RK. Preliminary phytochemical screening analysis and therapeutic

potential of *Tecoma stans* (L.). *Int. J. Appl. Chem*. **2017**, *13*, 129-34.

[15] Kumar KG, Boopathi T. An updated overview on pharmacognostical and pharmacological screening of *Tecoma stans*. *PharmaTutor*. **2018**, *6(1)*,38-49.

[16] Tariq H, Rafi M, Amirzada MI, Muhammad SA, Yameen MA, Mannan A, Ismail T, Shahzadi I, Murtaza G, Fatima N. Photodynamic cytotoxic and antibacterial evaluation of *Tecoma stans* and *Narcissus tazetta* mediated silver nanoparticles. *Arab. J. Chem*. **2022**, *15(3)*, 103652.

[17] Robinson JP, Suriya K, Subbaiya R, Ponmurugan P. Antioxidant and cytotoxic activity of *Tecoma stans* against lung cancer cell line (A549). *Braz. J. Pharm. Sci*. **2017,** 53.

[18] Hong X, Ajat M, Fakurazi S, Noor AM, Ismail IS. Anti-inflammatory evaluation of *Scurrula ferruginea* (jack) danser parasitizing on *Tecoma stans* (L.) HBK in LPS/IFN-γ-induced RAW 264.7 macrophages. *J. Ethnopharmacol*. **2021**, *268*, 113647.

[19] K. Sunitha and M. Nagulu, "In vitro screening of immunomodulatory activity of methanolic leaves extract of *Tecoma stans*," *IRJPMS, Volume 2, Issue 2,* pp. 52-54, 2019.

[20] Gonçalves TP, Parreira AG, dos Santos Zanuncio VS, de Souza Farias K, da Silva DB, dos Santos Lima LA. Antibacterial and antioxidant properties of flowers from *Tecoma stans* (L.) Juss. ex Kunth (Bignoniaceae). *S. Afr. J. Bot*. **2022**, 144, 156-65.

[21] Gupta A, Behl T. Proposed mechanism of *Tecoma stans* in diabetes-associated complications. *The Natural Products Journal*. **2021,** *11(2)*,127-39.

[22] Sadananda TS, Jeevitha MK, Pooja KS, Raghavendra VB. Antimicrobial, antioxidant activity and phytochemical screening of *Tecoma stans* (L.) Juss. ex Kunth. *J. Phytol*. **2011**, *3(3*).

[23] Larbie C, Owusu Nyarkoh C, Owusu Adjei C. Phytochemical and safety evaluation of hydroethanolic leaf extract of *Tecoma stans* (L.) Juss. ex Kunth. *eCAM*. **2019**.

[24] Shabani S, Rabiei Z, Amini-Khoei H. Exploring the multifaceted neuroprotective actions of gallic acid: A review. *Int J Food Prop*. **2020**, *23(1)*,736-52.

[25] Gao J, Hu J, Hu D, Yang X. A role of gallic acid in oxidative damage diseases: A comprehensive review. *Nat. Prod. Commun*. **2019**, *14(8)*, 1934578X19874174.

[26] Jin L, Sun S, Ryu Y, Piao ZH, Liu B, Choi SY, Kim GR, Kim HS, Kee HJ, Jeong MH. Gallic acid improves cardiac dysfunction and fibrosis in pressure overload-induced heart failure. *Sci. Rep*. **2018,** *8(1)*,9302.

[27] Bai J, Zhang Y, Tang C, Hou Y, Ai X, Chen X, Zhang Y, Wang X, Meng X. Gallic acid: Pharmacological activities and molecular mechanisms involved in inflammation-related diseases. ***Biomed. Pharmacother***. **2021,** *133*, 110985.

[28] Shabani S, Rabiei Z, Amini-Khoei H. Exploring the multifaceted neuroprotective actions of gallic acid: A review. ***Int J Food Prop***. **2020,** *23(1)*,736-52.

[29] Kumar S, Baldi A, Sharma DK. Phytosomes: a modernistic approach for novel herbal drug delivery-enhancing bioavailability and revealing endless frontier of Phytopharmaceuticals. *J. Dev. Drugs*. **2019**, *9*, 1-8.

[30] Sukhbir S, Yashpal S, Sandeep A. Development and statistical optimization of nefopam hydrochloride loaded nanospheres for neuropathic pain using Box–Behnken design. *SPJ*. **2016,** *24(5)*,588-99.

[31] El-Menshawe SF, Ali AA, Rabeh MA, Khalil NM. Nanosized soy phytosome-based thermogel as topical anti-obesity formulation: an approach for acceptable level of evidence of an effective novel herbal weight loss product. *Int J Nanomedicine*. **2018**, *13* 307.

[32] Sharma S, Sahu AN. Development, characterization, and evaluation of hepatoprotective effect of *Abutilon indicum* and *Piper longum* phytosomes. *Pharmacogn. Res*. **2016,** *8(1)*, 29.

[33] Rathee S, Kamboj A. Optimization and development of antidiabetic phytosomes by the Box–Behnken design. *J. Liposome Res*. **2018**, *28(2)*, 161-72.

[34] Sahu AR, Bothara SB. Formulation and evaluation of phytosome drug delivery system of *Boswellia serrata* extract. *Int J Res Med*. **2015,** *4(2)*, 94-9.
[35] Udapurkar PP, Bhusnure OG, Kamble SR. Diosmin Phytosomes: development, optimization and physicochemical characterization. *Indian J Pharm Educ Res*. **2018**, *52(4)*, S29-36.
[36] Gulia R, Singh S, Arora S, Sharma N. Development and optimization of Hydrotropic solid dispersion of dexlansoprazole using central composite design approach. *J. Integr. Sci. Technol*. **2023**, *11(4)*, 559-.
[37] Islam N, Irfan M, Hussain T, Mushtaq M, Khan IU, Yousaf AM, Ghori MU, Shahzad Y. Piperine phytosomes for bioavailability enhancement of domperidone. *J. Liposome Res*. **2022**, *32(2)*, 172-80.
[38] Singh RP, Ramakant N. Preparation and evaluation of phytosome of lawsone. *IJPSR*. **2015**, *6(12)*, 5217-26.
[39] Ha ES, Park H, Lee SK, Sim WY, Jeong JS, Baek IH, Kim MS. Pure trans-resveratrol nanoparticles prepared by a supercritical antisolvent process using alcohol and dichloromethane mixtures: effect of particle size on dissolution and bioavailability in rats. *Antioxidants*. **2020**, *9(4)*, 342.
[40] Sharma N, Arora S, Madan J. Nefopam hydrochloride loaded microspheres for post-operative pain management: synthesis, physicochemical characterization and in-vivo evaluation. *Artif Cells Nanomed Biotechnol*. **2018**, *46(1)*, 138-46.
[41] Freag MS, Saleh WM, Abdallah OY. Self-assembled phospholipid-based phytosomal nanocarriers as promising platforms for improving oral bioavailability of the anticancer celastrol. *Int. J. Pharm.* **2018**, *535(1-2)*,18-26.
[42] Kocher A, Schiborr C, Behnam D, Frank J. The oral bioavailability of curcuminoids in healthy humans is markedly enhanced by micellar solubilisation but not further improved by simultaneous ingestion of sesamin, ferulic acid, naringenin and xanthohumol. *J. Funct. Foods*. **2015**, *14*, 183-91.
[43] Shriram RG, Moin A, Alotaibi HF, Khafagy ES, Al Saqr A, Abu Lila AS, Charyulu RN. Phytosomes as a plausible nano-delivery system for enhanced oral bioavailability and improved hepatoprotective activity of silymarin. *Pharmaceuticals*. **2022**, *15(7)*, 790.
[44] Sharma S, Sahu AN. Development, characterization, and evaluation of hepatoprotective effect of *Abutilon indicum* and *Piper longum* phytosomes. *Pharmacogn. Res*. **2016**, *8(1)*, 29.
[45] Saudagar WS, Sidram GP, Baburo GS, Agarwal G, Agarwal S, Gadgeppa BO. Development and characterization of *Terminalia arjuna* Phospholipid complex and its tablet formulation by QbD approach. *Int. J. Life Sci. Pharma Res*. **2021**, *11(3)*, P14-28.
[46] Gahandule MB, Jadhav SJ, Gadhave MV, Gaikwad DD. Formulation and development of hepato-protective butea monosperma-phytosome. *Int J Res Pharm Pharm Sci*. **2016**, *1(4)*, 21-7.
[47] S, Mubarak H, Ramadon D. Cosmetic serum containing grape (*Vitis vinifera* L.) seed extract phytosome: Formulation and in vitro penetration study. *J Young Pharm*. **2018**, *10(2s)*, S51.
[48] Direito R, Reis C, Roque L, Gonçalves M, Sanches-Silva A, Gaspar MM, Pinto R, Rocha J, Sepodes B, Rosário Bronze M, Eduardo Figueira M. Phytosomes with persimmon (*Diospyros kaki* l.) extract: Preparation and preliminary demonstration of in vivo tolerability. *Pharmaceutics*. **2019**, *11(6)*, 296.
[49] Agarwal A, Kharb V, Saharan VA. Process optimisation, characterisation and evaluation of resveratrol-phospholipid complexes using box-behnken statistical design. *Int. Curr. Pharm. J.* **2014**, *3(7)*, 301-8.
[50] Singh A, Arora S, Singh TG. Development and optimization of *Andrographis paniculata* extract-loaded phytosomes using box-behnken design approach. *J. Integr. Sci. Technol*. **2023**, *11(4)*, 558.
[51] Singh RP, Gangadharappa HV, Mruthunjaya K. Phytosome complexed with chitosan for gingerol delivery in the

treatment of respiratory infection. *Eur J Pharm Sci*. **2018**, *122*, 214-29.

[52] Peanparkdee M, Yooying R. Enhancement of solubility, thermal stability and bioaccessibility of vitexin using phosphatidylcholine-based phytosome. *NFS Journal*. **2023,** *31*, 28-38.

[53] Chen X, Fan X, Li F. Development and evaluation of a novel diammonium glycyrrhizinate phytosome for nasal vaccination. *Pharmaceutics*. **2022,** *14(10)*,2000.

[54] Zhang J, Tang Q, Xu X, Li N. Development and evaluation of a novel phytosome-loaded chitosan microsphere system for curcumin delivery. *Int. J. Pharm*. **2013,** *448(1)*, 168-74.

[55] Hou Z, Li Y, Huang Y, Zhou C, Lin J, Wang Y, Cui F, Zhou S, Jia M, Ye S, Zhang Q. Phytosomes loaded with mitomycin C–soybean phosphatidylcholine complex developed for drug delivery. *Mol. Pharm*. **2013,** *10(1)*, 90-101.

[56] Sabzichi M, Hamishehkar H, Ramezani F, Sharifi S, Tabasinezhad M, Pirouzpanah M, Ghanbari P, Samadi N. Luteolin-loaded phytosomes sensitize human breast carcinoma MDA-MB 231 cells to doxorubicin by suppressing Nrf2 mediated signalling. *Asian Pac J Cancer Prev*. **2014**, *15(13)*, 5311-6.

[57] Freag MS, Elnaggar YS, Abdallah OY. Lyophilized phytosomal nanocarriers as platforms for enhanced diosmin delivery: optimization and ex vivo permeation. *Int. J. Nanomedicine*. **2013**, 2385-97.

[58] Pasala PK, Uppara RK, Rudrapal M, Zothantluanga JH, Umar AK. Silybin phytosome attenuates cerebral ischemia-reperfusion injury in rats by suppressing oxidative stress and reducing inflammatory response: In vivo and in silico approaches. *J. Biochem. Mol. Toxicol*. **2022,** *36(7)*, e23073.

[59] Huang Z, Brennan CS, Zhao H, Liu J, Guan W, Mohan MS, Stipkovits L, Zheng H, Kulasiri D. Fabrication and assessment of milk phospholipid-complexed antioxidant phytosomes with vitamin C and E: A comparison with liposomes. *Food Chem*. **2020**, *324*, 126837.

[60] Murugesan MP, Ratnam MV, Mengitsu Y, Kandasamy K. Evaluation of anti-cancer activity of phytosomes formulated from Aloe vera extract. *Mater Today*. **2021,** *42*, 631-6.

[61] Lu M, Qiu Q, Luo X, Liu X, Sun J, Wang C, Lin X, Deng Y, Song Y. Phyto-phospholipid complexes (phytosomes): A novel strategy to improve the bioavailability of active constituents. *Asian J. Pharm. Sci*. **2019,** *14(3)*, 265-74.

[62] Das MK, Kalita B. Design and evaluation of phyto-phospholipid complexes (phytosomes) of rutin for transdermal application. *J. Appl. Pharm. Sci*. **2014,** *4(10)*, 051-7.

[63] Karole S, Gupta GK. Preparation and evaluation of phytosomes containing ethanolic extract of leaves of *Bombax ceiba* for hepatoprotective activity. *Evaluation*. **2019**, *6(2)*, 1-5.

[64] Mazumder A, Dwivedi A, Fox LT, Brümmer A, du Preez JL, Gerber M, du Plessis J. In vitro skin permeation of sinigrin from its phytosome complex. *J. Pharm. Pharmacol*. **2016,** *68(12)*, 1577-83.